Multi - component line emission in young stars. Spectroscopy and Interferometry

L.V. Tambovtseva[1,3], V.P. Grinin[1,2,3], G. Weigelt[3], D. Schertl[3], K.-H. Hofmann[3], R. Garcia-Lopez[4], A. Caratti o Garatti[4]

[1]Pulkovo Astronomical Observatory , St. Petersburg, Russia, [2]The Sobolev Astronomical Institute of the St. Petersburg University, St. Petersburg, Russia, [3]Max-Planck-Institut für Radioastronomie, Bonn, Germany, [4]Dublin Institute for Advanced Studies, Dublin, Ireland

CONTENT

1. A short report on hydrogen emission line modeling in Herbig AeBe stars (LT)

   - Accreting and outflowing regions emitting in the hydrogen lines
   - Non-LTE calculations, basic assumptions, computation of the line profiles
   - A mutual reproduction of the IR interferometric observables and line profiles. The Brγ line.

2. Topics and problems to discuss: (VG)

   - How to obtain a restriction to the model parameters
   - How to improve models
   - A difference in the models for the low-mass (TTSs), intermediate-mass (HAEBEs) and massive stars

Herbig Ae star: line emitting regions

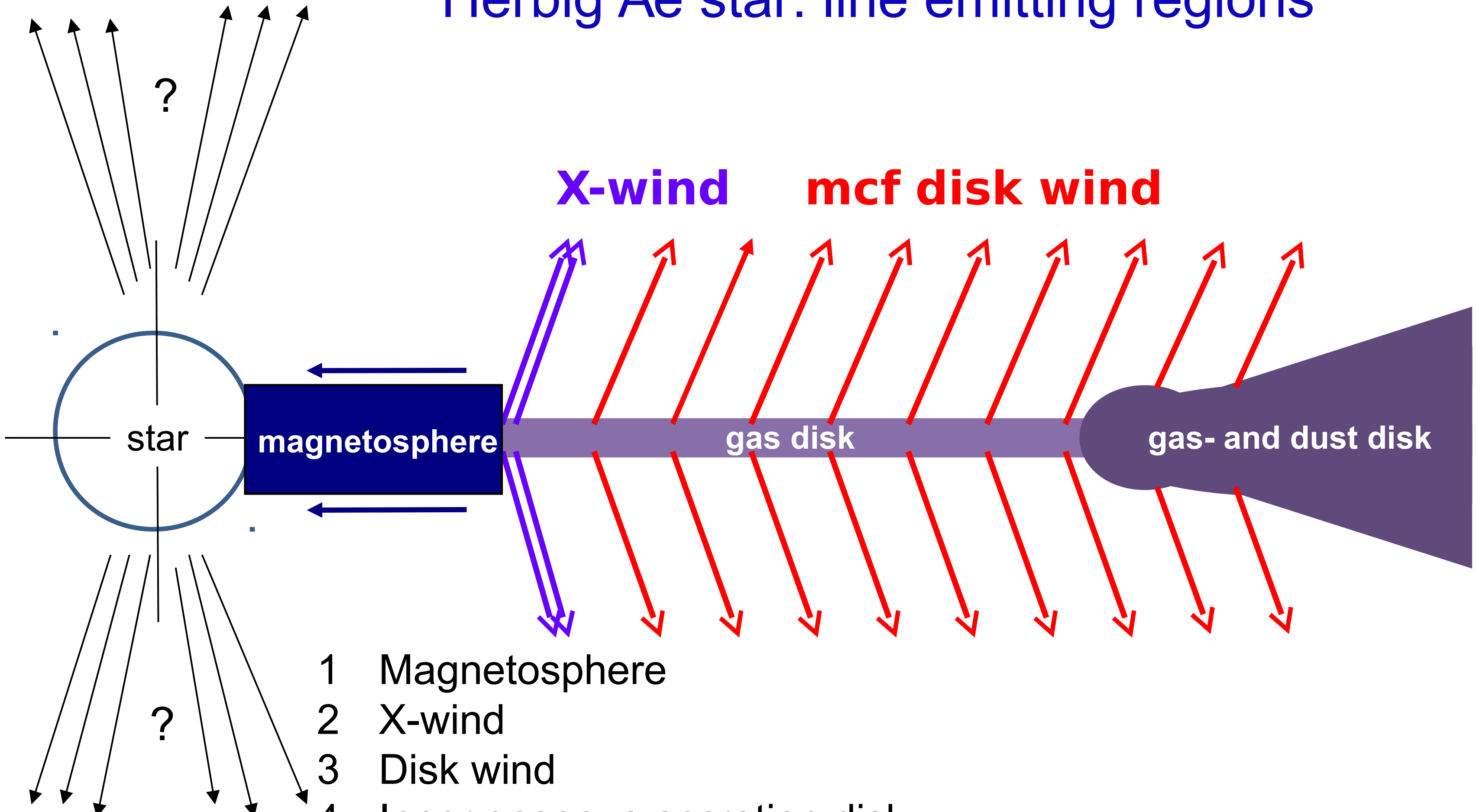

1 Magnetosphere
2 X-wind
3 Disk wind
4 Inner gaseous accretion disk

Disk wind: (TTSs)

1 Magneto-centrifugal (mcf) disk wind (Blandford & Payne 1982)
1 X-wind (Shu et al. 1994)
2 Conical wind (Romanova et al. 2009)
3 Disk wind due to photoevaporation (e.g.,Gorti & Hollenbach 2008)

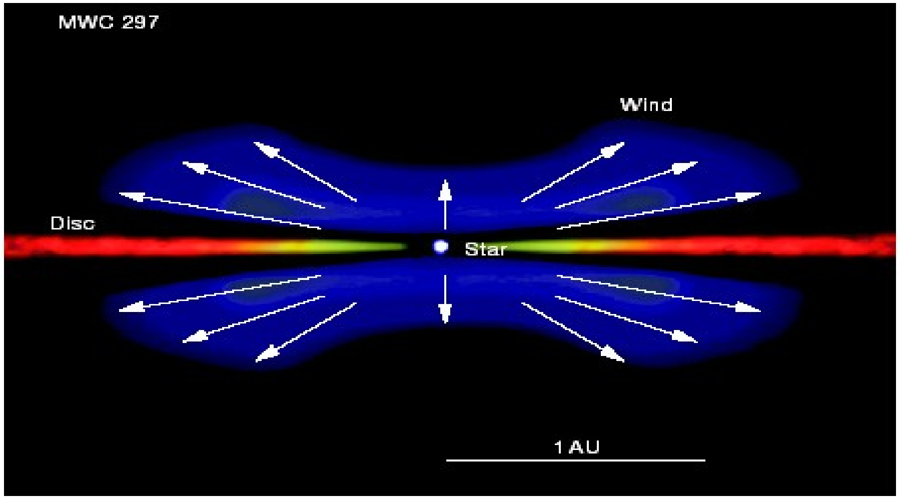

Mass continuity equation for each streamline

$$\dot{m}_1 \quad \dot{m}_2 \quad \cdots\cdots \quad \dot{m}_N$$

$$\dot{m}_i = 4\pi\rho v_p(l)\, l^2$$

$$\boxed{\begin{aligned} u(\omega) &= u_K(\omega_i)\,(\omega/\omega_i)^{-1}\,, \\ v(l) &= v_0 + (v_\infty - v_0)\,(1 - l_i/l)^\beta\,, \end{aligned}}$$

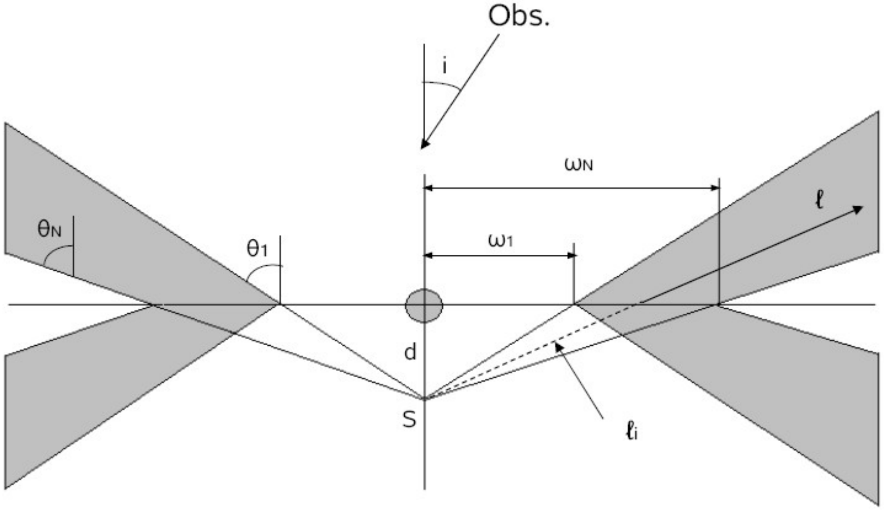

$$\dot{m}_w(\omega) \sim \omega^{-\gamma}$$

the total mass-loss rate:

$$\dot{M}_w = 2\int_{\omega_1}^{\omega_N} \dot{m}_w(\omega)\, 2\,\pi\,\omega\, d\omega$$

Shlosman & Vitello (1993) (cataclysmic variables)
Kurosawa et al. (2006) (TTSs)
Murray & Chiang (1997) (galactic nuclei)
Grinin & Tambovtseva (2011) (HAEBEs)

Radiative transfer codes:

Grinin & Katysheva 1980
Grinin & Mitskevich 1990
Tambovtseva et al. 2001

Radiative transition probabilities (Gershberg & Shnol 1974),
Collision transition probabilities (Johnson 1972, Scholz et al. 1990)

$$\boxed{\frac{dn_i}{dt} = R_i + Q_i = 0,}$$

system of the stationary equations

$$\boxed{\begin{aligned} R_i = -n_i \left(\sum_{j=i}^{i-1} (A_{ij} + B_{ij} J_{ij}) + \sum_{k=i+1}^{\infty} B_{ik} J_{ik} + B_{ic} W\, J^{\star}_{ic} \right) + \\ + \sum_{k=i+1}^{\infty} n_k (A_{ki} + B_{ki} J_{ik}) + \sum_{j=1}^{i-1} n_j B_{ji} J_{ij}, \end{aligned}}$$

Radative and collision excitation and de-excitaton of the i-th level

$$i = 1,2,3 \ldots N_{atom} \qquad (15)$$

$$\boxed{\begin{aligned} Q_i = -n_i \left(n_e (q_{ic} + \sum_{i \neq j} q_{ij}) + B_{ci} W\, J^{\star}_{ic} \right) + \\ + n_e \sum_{j \neq i}^{\infty} n_j q_{ji} + n_e n^+ C_i + n_e^2 n^+ Q_{ci} \end{aligned}}$$

Radiative transition probabilities (Gershberg & Shnol 1974),
Collision transition probabilities (Johnson 1972, Scholz et al. 1990)

Intensity of the radiation:

$$J_{ik} = (1- < \beta_{ik} >)S_{ik} + J^{\star}_{ik} W \beta^{\star}_{ik}$$

Source function:

$$S(r) = \frac{2hv^3}{c^2} \left(\frac{n_k(r)}{n_i(r)} \frac{g_i}{g_k} - 1 \right)^{-1}$$

Mean escape probability of the quantum in the line *ik* from the given point of the medium:

$$< \beta_{ik}(l,\theta) > = \int \beta_{ik}(r,l,\mathsf{s}) \frac{d\Omega}{4\pi} ,$$

$$\beta_{ik}(l,\theta,\mathsf{s}) = \frac{1 - e^{-\tau_{ik}}}{\tau_{ik}}$$

The integral is taken over all solid angles Ω (ℓ,θ)

The effective optical depth of the emitting region at the point with co-ordinates (ℓ,θ):

$$\tau_{ik}(l,\theta,\mathsf{s}) = \kappa_{ik}(l,\theta)\, v_t\, |dv_{\mathsf{s}}/ds|^{-1}$$

SEI = Sobolev + Exact Integration

$$I_w(\nu) = \int_A I_w(\nu,x,y)\,dx\,dy$$

$$I_w(\nu,x,y) = \int_{z_{min}}^{z_{max}} S(\mathbf{r}) \phi(\nu - \nu_0 \frac{\mathsf{v}_z(\mathbf{r})}{c})\, e^{-\tau(\nu,\mathbf{r})} \kappa(\mathbf{r})\, dz$$

The velocity gradient in the co-moving frame at the arbitrary direction **s**

The Sobolev length:

$$s_0 = v_{th} / \left| dv_{\vec{s}} / ds \right| << r$$

Spherically symmetric stellar wind:

$$\frac{dv_{\vec{s}}}{ds} = \frac{dv}{dr}\mu^2 + \frac{v}{r}\left(1-\mu^2\right) \qquad \mu = \cos\theta$$

Axially symmetric outflow / disk accretion

$$\frac{dv_{\vec{s}}}{ds} = \left(\frac{dv}{dr} - \frac{v}{r}\right)\cos^2\theta + \frac{v}{r} + \left(\frac{du}{dr} - \frac{u}{r}\right)\sin\theta\cos\theta$$

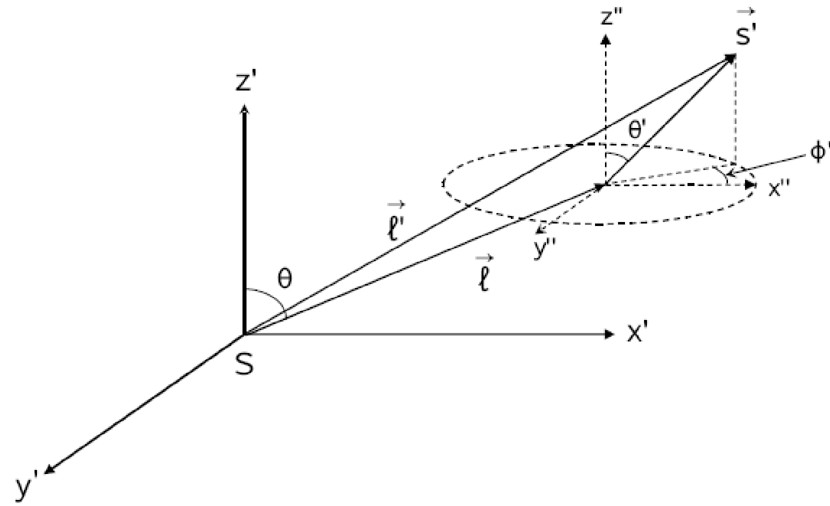

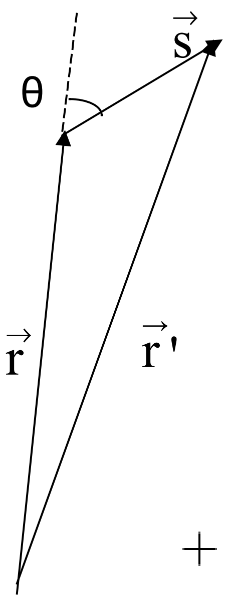

$$v_z = v\cos\theta$$

$$v_\omega = v\sin\theta$$

Axially symmetric disk wind:

$$\frac{dv_{\mathbf{s}}}{ds} = \frac{\partial u}{\partial \omega}\sin\theta'\cos\phi'\sin\phi' + \frac{\partial u}{\partial z}\cos\theta'\sin\phi' - \frac{u}{\omega}\sin\phi'\cos\phi' + \frac{\partial v_z}{\partial z}\cos^2\theta'$$
$$+ \frac{\partial v_z}{\partial \omega}\sin\theta'\cos'\theta'\cos\phi' + \frac{\partial v_\omega}{\partial \omega}\sin\theta'\cos^2\phi' + \frac{v_\omega}{\omega}\sin^2\phi' + \frac{\partial v_\omega}{\partial z}\cos\theta'\cos\phi',$$

Grinin and Tambovtseva 2011

Safier 1993

ω = 0.1AU

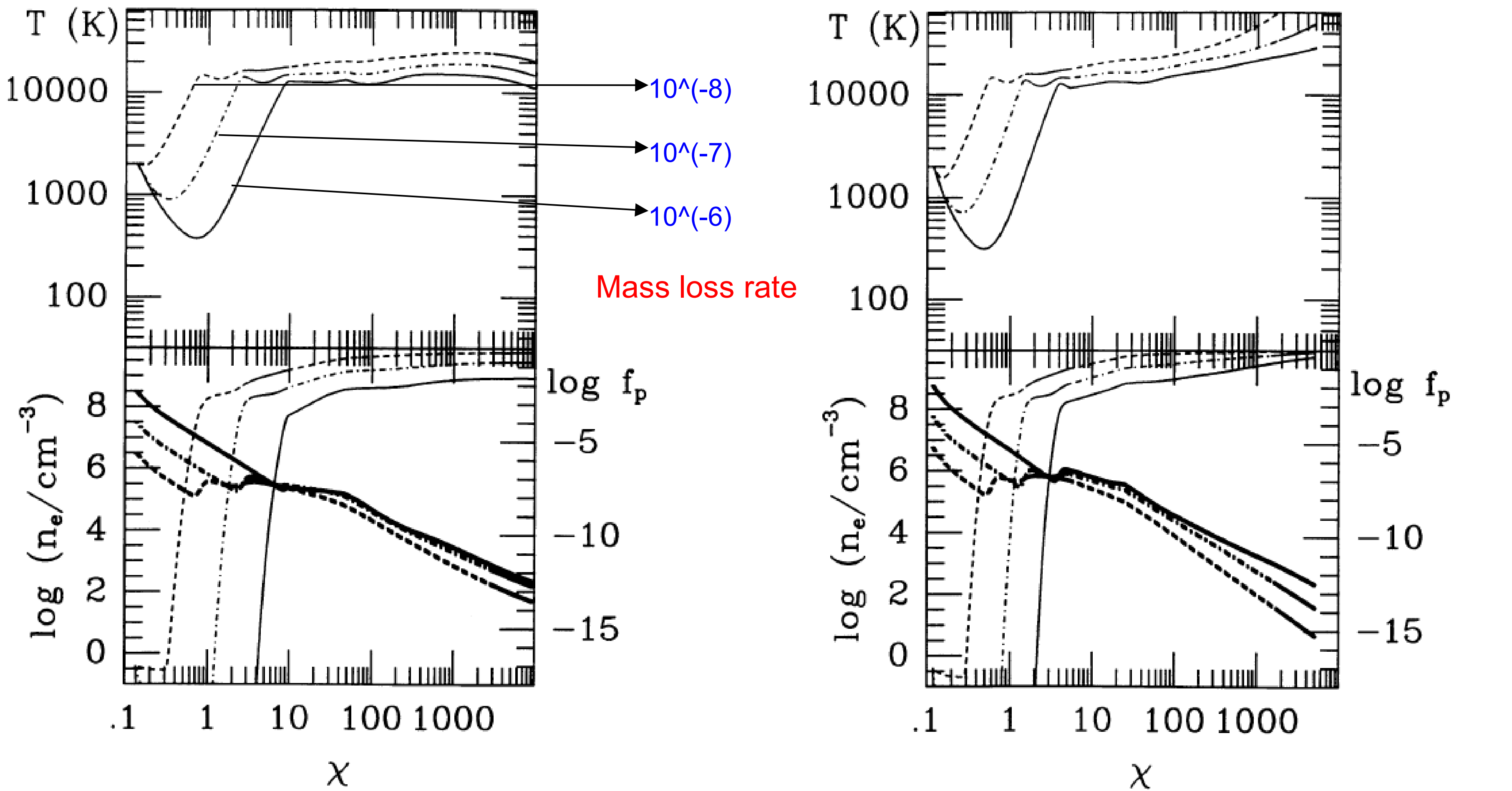

FIG. 6a FIG. 6b

FIG. 6.—(*a*) Dependence of the wind thermal structure on $\dot{M}_{out}$ for case C. The results correspond to the $\varpi_0 = 0.1$ AU flowline. *Top*: gas temperature; *bottom*: ectron number density (*heavy lines*; *left-hand scale*) and the hydrogen ionization fraction (*light lines*; *right-hand scale*). *Solid line*: $\dot{M}_{out} = 10^{-6}\ M_\odot\ yr^{-1}$; *dash-dot ne*: $\dot{M}_{out} = 10^{-7}\ M_\odot\ yr^{-1}$; *dashed line*: $\dot{M}_{out} = 10^{-8}\ M_\odot\ yr^{-1}$. (*b*) Dependence of the wind thermal structure on $\dot{M}_{out}$ for case G. The notation is the same as in (*a*).

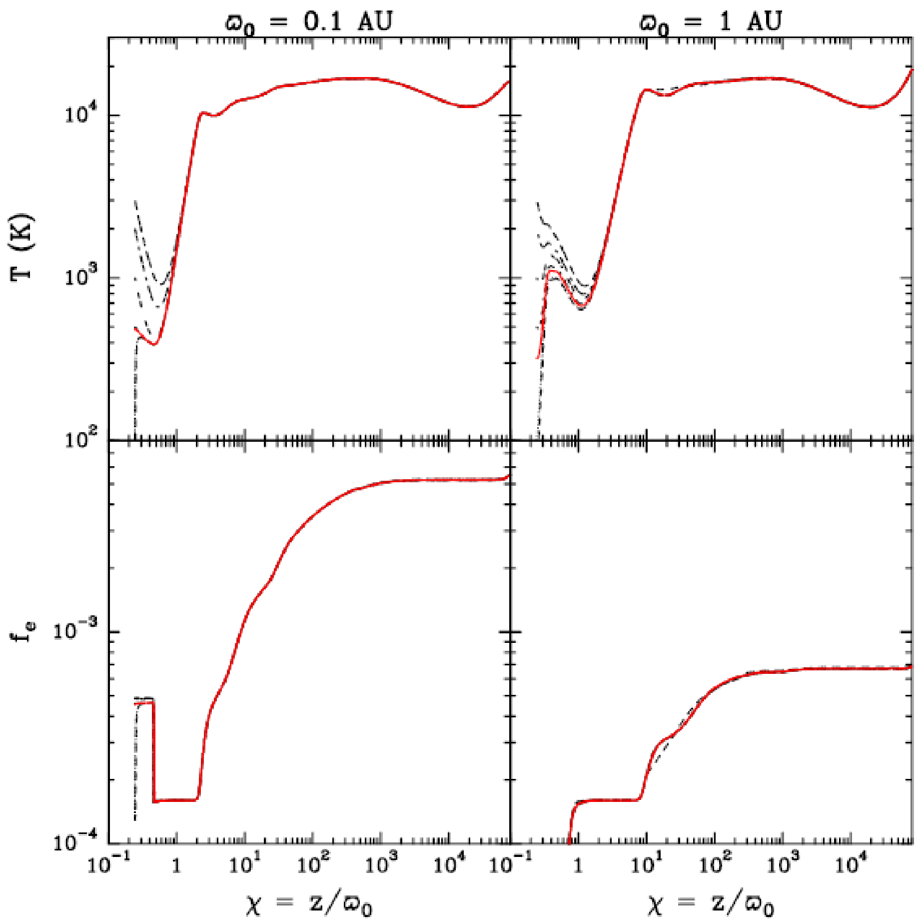

Fig. C.3. Effect of initial temperature on the thermal evolution for model B, $\dot{M}_{acc} = 10^{-6}\ M_\odot\ yr^{-1}$. The several initial temperatures are in dashed 50 K, 100 K, 500 K, 1000 K, 2000 K and 3000 K. In solid we plot the solution obtained by our standard initial conditions. Note that the almost vertical evolution of the temperature for very low initial temperatures is not an artifact. The field line anchored at $\varpi_0 = 0.1$ AU crosses the sublimation surface at $\chi \simeq 0.5$.

Garcia et al. 2001

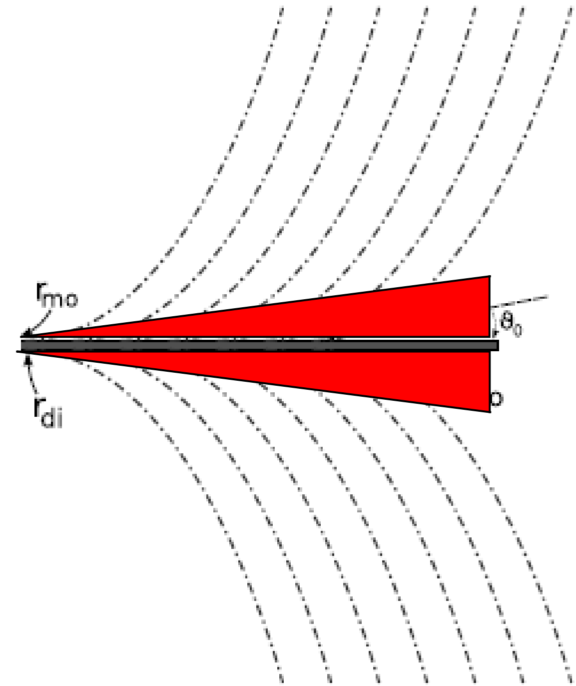

1) To ignore the base of the wind because of the low gas temperature

1) The approximation of “straight lines” is not so rough

$$V_\infty = f U_K$$

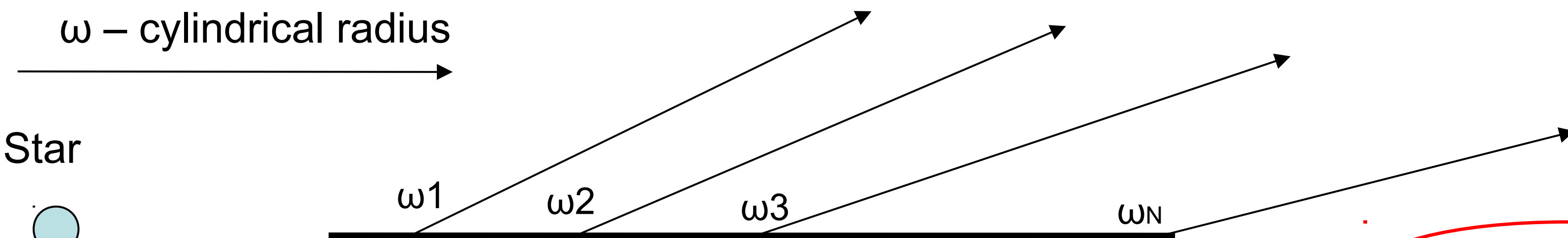

$V_{\infty 1} = 3U_{K1}$ $V_{\infty 2} = 3U_{K2}$ $V_{\infty 3} = 3U_{K3}$ $V_{\infty N} = 3U_{KN}$

f = const = 3

$V_{\infty 1} = 3U_{K1}$ $V_{\infty 1} = 2U_{K1}$ $V_{\infty 1} = 1U_{K1}$ $V_{\infty 1} = 0.5U_{K1}$

f ≠ const

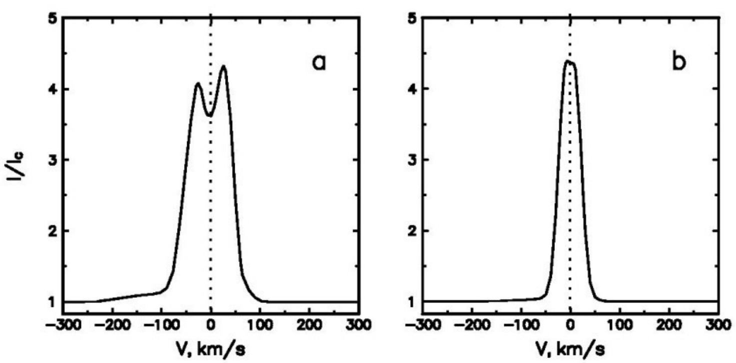

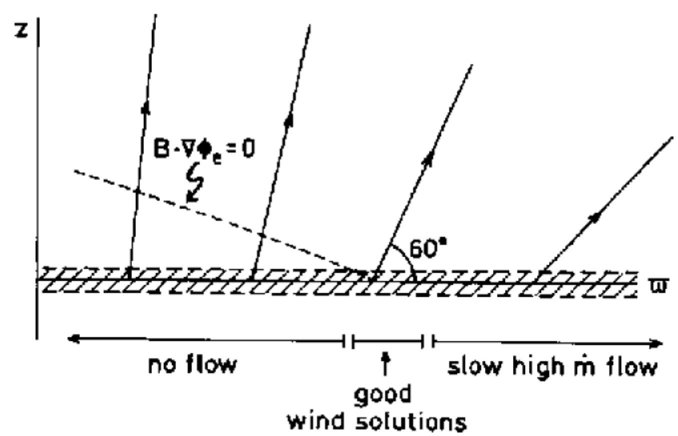

f = 2 f = 3,2,1… etc.

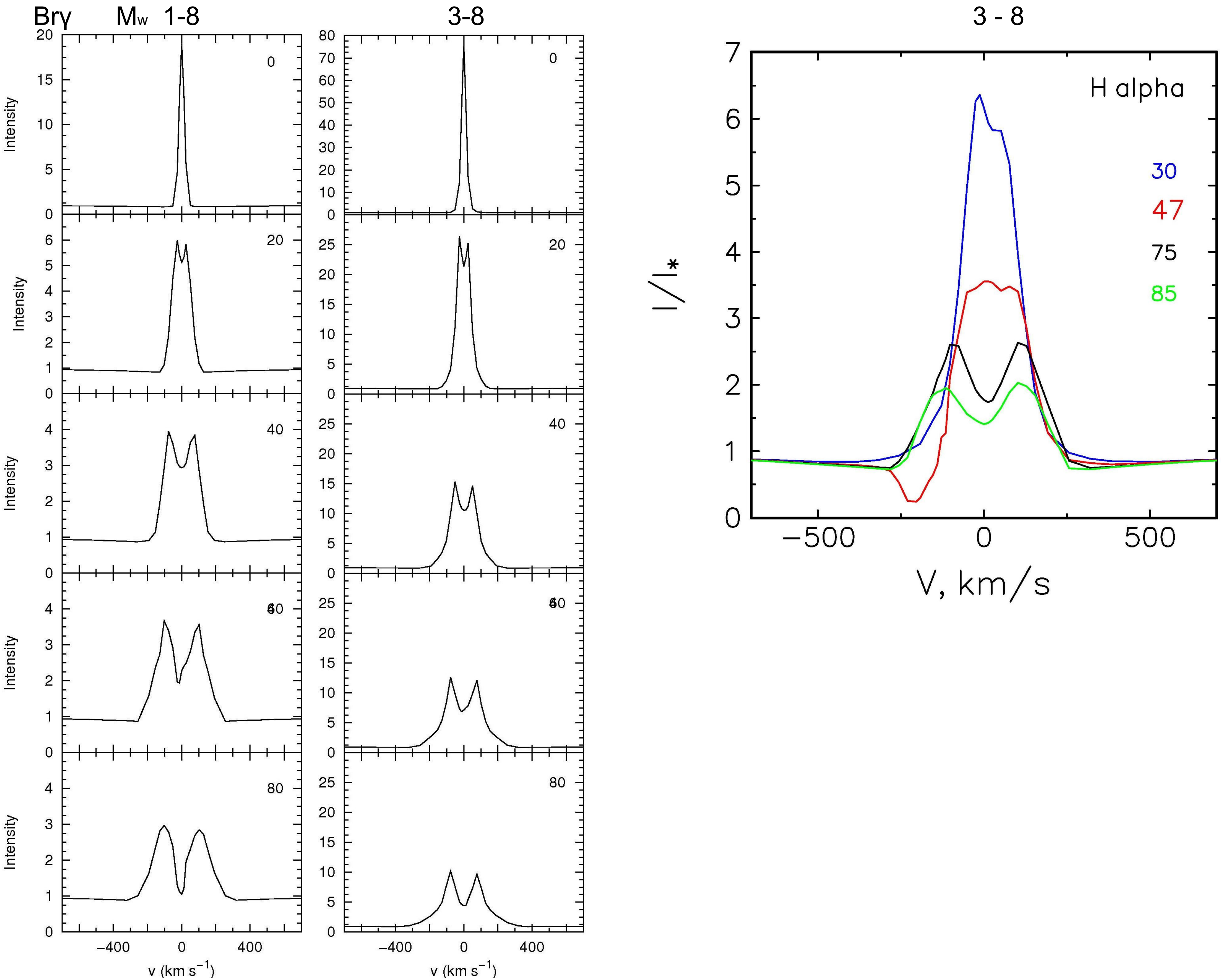

Brγ
M_w 1-8
3-8
3 - 8
Intensity
v (km s^{-1})
0
20
40
60
80
H alpha
30
47
75
85
I/I_*
V, km/s

Two approximations for the magnetosphere structure

Flat-like magnetosphere : rotating gas, free-fall motion

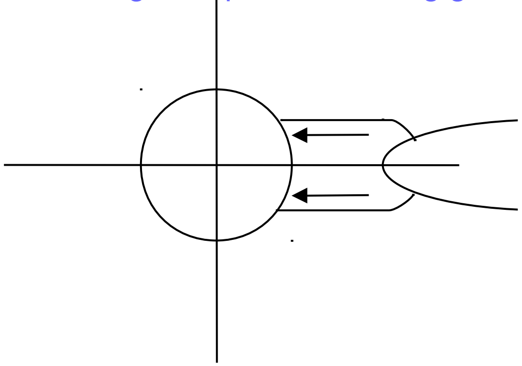

boundary layer accretion

Cone-like magnetosphere: rotating gas within two thin cones; motion to the poles

magnetospheric accretion

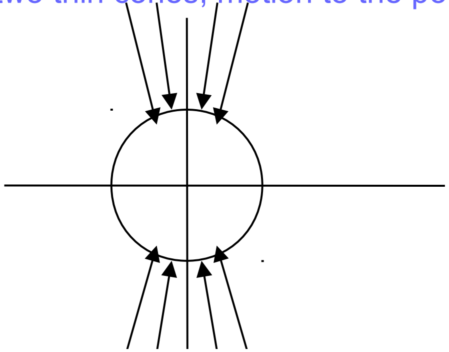

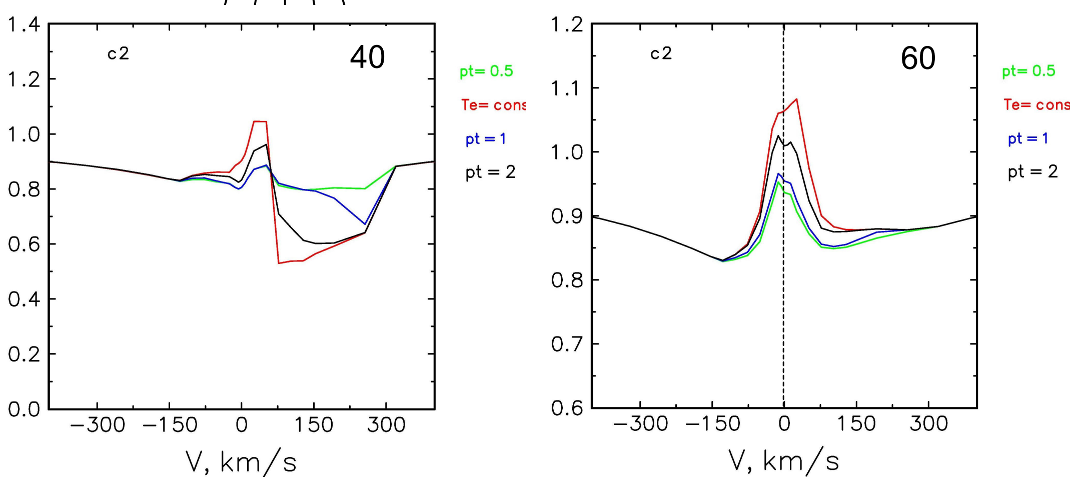

Populations of the atomic levels are controlled by

Star radiation + gas kinematics

Gas kinematics

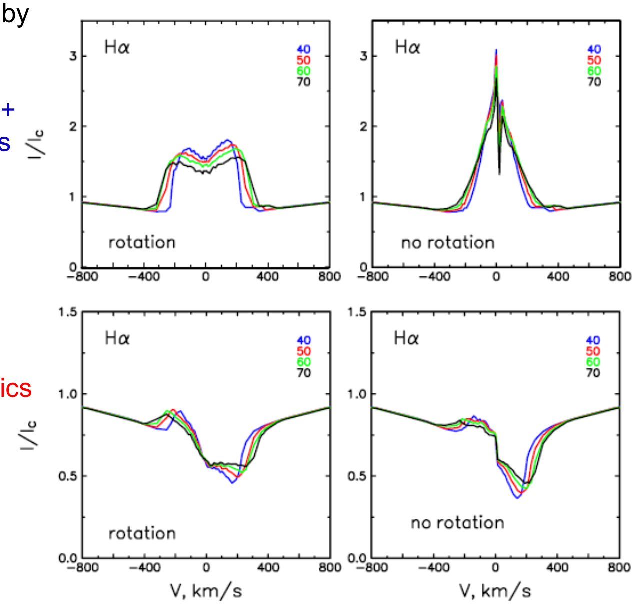

Fig. 10. *Top*: Hα line profiles of the magnetospheric accretion model MS1 with (*left*) and without (*right*) rotation and $\dot{M}_{acc} = 1\times10^{-7}\ M_{\odot}\ yr^{-1}$. The numbers in the panel indicate the inclination angles *i*. *Bottom*: the same for model MS2.

Star radiation + gas kinematics

Gas kinematics

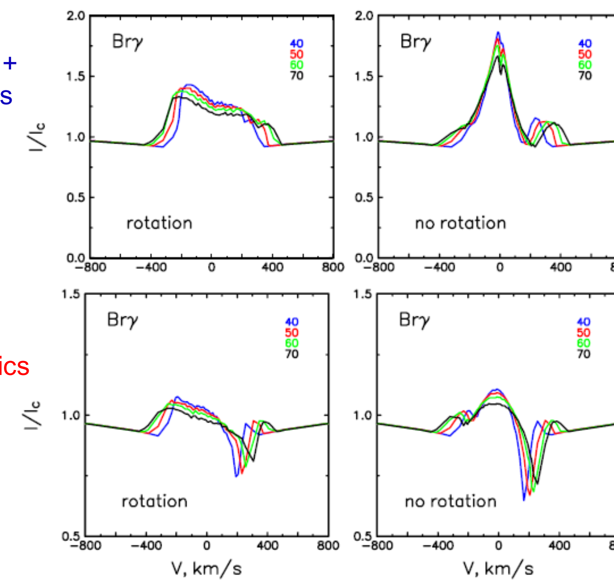

VLTI/AMBER spectro-interferometry of the Herbig Be star MWC 297 with spectral resolution 12 000 ⋆

2011

G. Weigelt[1], V. P. Grinin[2,3], J. H. Groh[1], K.-H. Hofmann[1], S. Kraus[4], A. S. Miroshnichenko[5], D. Schertl[1], L. V. Tambovtseva[2], M. Benisty[6], T. Driebe[7], S. Lagarde[8], F. Malbet[9], A. Meilland[1,8], R. Petrov[8], and E. Tatulli[9]

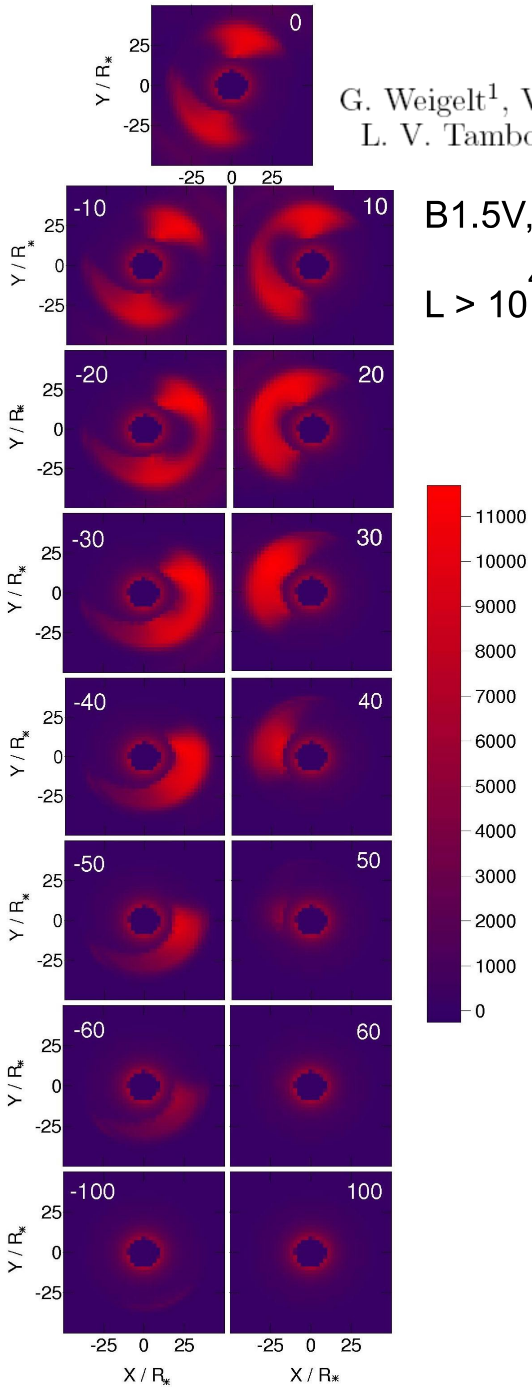

B1.5V, $M=10M_o$

$R=6R_o$

$L > 10^4 L_o$

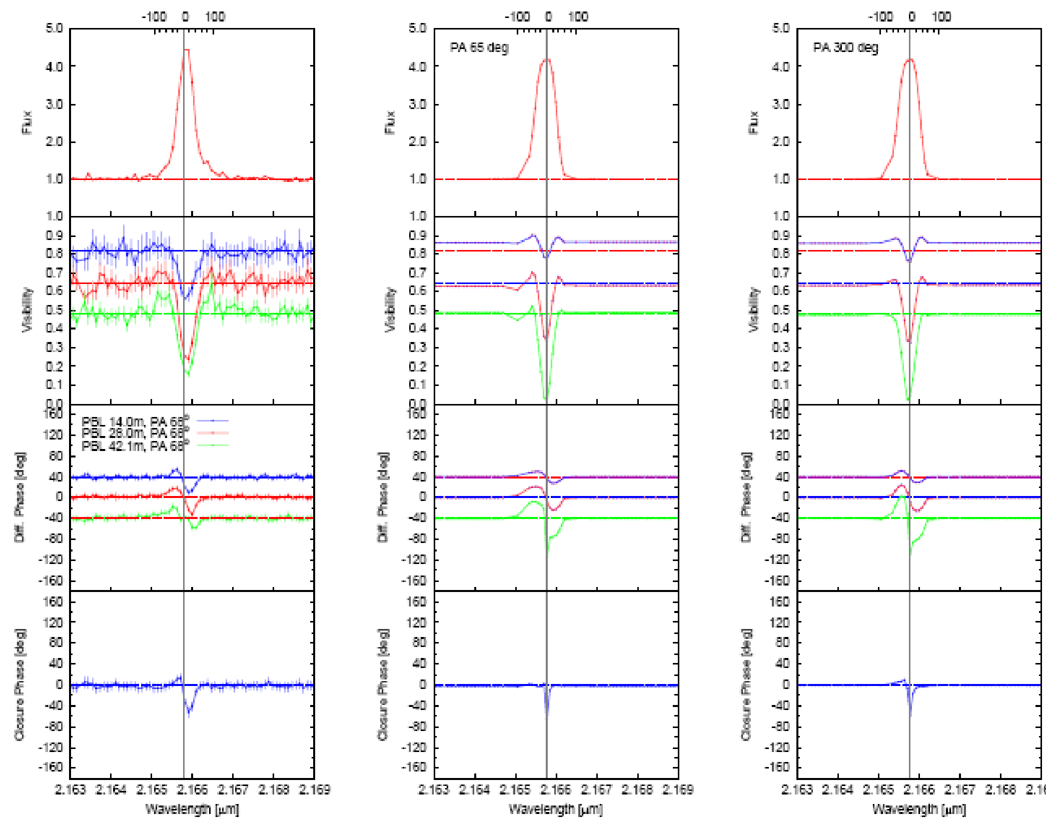

Fig. 8. Comparison of the observations (left panel, see Fig. 1) with the corresponding model quantities of model 5 fo different PAs of the model image (middle and right panel; the model quantities are calculated for AMBER's spectral resoluti $R = 12\,000$, as discussed in Section A.3 and Fig. A.4). The middle and right panels show the dependence of the interferon observables (spectrum, visibilities, wavelength-differential phases, and closure phases) of our best disk-wind model 5 (disk- emitting region, continuum accretion disk, plus central star; see Tables 3 and A.1) on the wavelength across the Brγ line f inclination angle of $i = 20°$, clock-wise motion of the disk wind, and for two different PAs of the projected disk polar ax the sky: 65° (middle) and 300° (right). Several other PAs which are also approximately in agreement with the observation discussed in the text and in Figs. A.5 and A.6. The detailed dependence of the interferometric observables on the PA is prese in Figs. A.5 and A.6.

MWC 275
HD 163296
Ae Herbig

i = 38°

A&A proofs: manus

$SpT^{(1)}$	$T_{eff}^{(2)}$ (K)	$d^{(3)}$ (pc)	$R_*^{(2)}$ ($R_\odot$)	$M_*^{(2)}$ ($M_\odot$)	$\dot{M}_{acc}^{(4)}$ ($10^{-7} M_\odot/yr$)	$\dot{M}_{out}^{(5)}$ ($M_\odot/yr$)
A1V	9250	119±11	2.3	2.2	0.8 – 4.5*	5×10^{-10} – 2×10^{-7} **

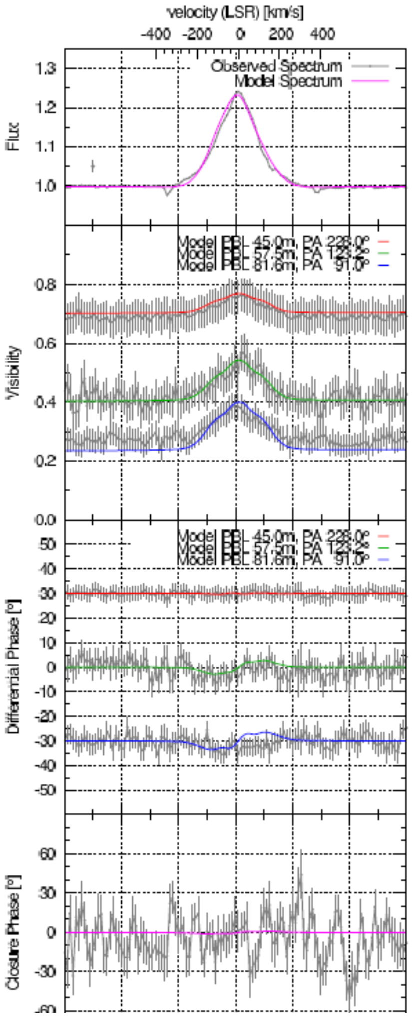

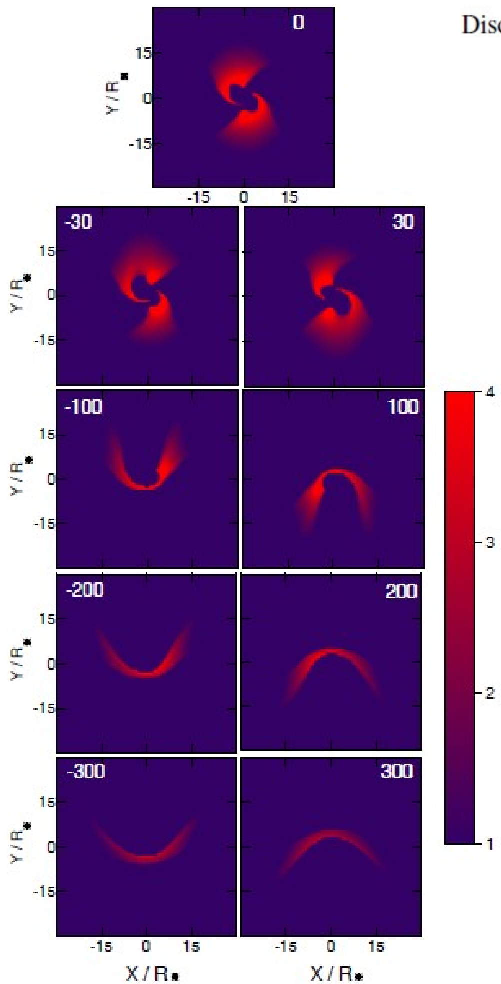

Disc wind model parameters

Parameters^a	Range^b	MW6^b
Temperature (K)	8000 – 10 000	10 000
Half opening angle (θ)	30° – 45°	45°
Inner radius ($\omega_1(R_*)$)	2 – 3	2.0 (0.02 AU)
Outer radius ($\omega_N(R_*)$)	4 – 30	4.0 (0.04 AU)
Acceleration parameter (β)	1 – 7	5
Mass load parameter (γ)	1 – 5	3
Mass loss rate ($\dot{M}_w(M_\odot/yr)$)	10^{-8} – 10^{-7}	5×10^{-8}

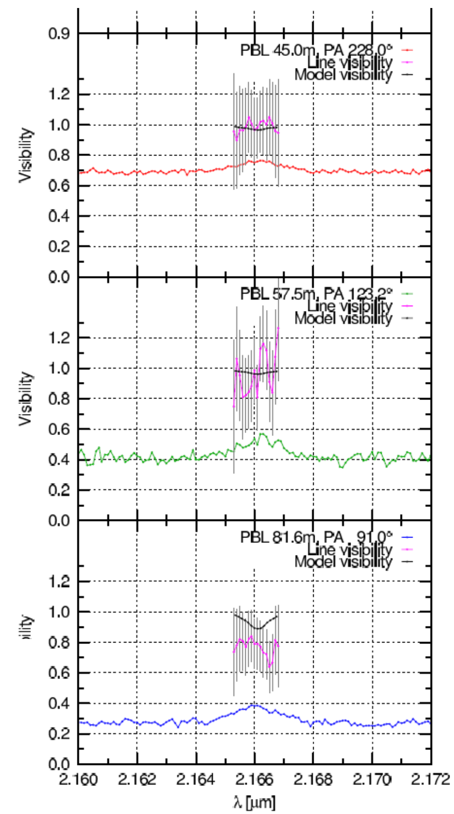

Probing the accretion-ejection connection with VLTI/AMBER

High spectral resolution observations of the Herbig Ae star HD163296 ★

R. Garcia Lopez[1,4], L.V. Tambovtseva[1,2], D. Schertl[1], V.P. Grinin[1,2,3], K.-H Hofmann[1], G. Weigelt[1], and A. Caratti o Garatti[1,4]

AMBER/VLTI high spectral resolution observations of the Brγ emitting region in HD 98922

A compact disc-wind launched from the inner disc region ★

A. Caratti o Garatti[1,2], L.V. Tambovtseva[2,3], R. Garcia Lopez[1,2], S. Kraus[4], D. Schertl[2], V.P. Grinin[2,3,5], G. Weigelt[2], and K.-H. Hofmann[2]

HD 98922
Be Herbig

i = 20°

Table 2. HD 98922 stellar and disc parameters

Stellar Parameter	Value	Reference
Distance	$440\pm^{60}_{50}$ pc	1
$T_{\rm eff}$	10 400±200 K	1,2
$SpType$	B9V	1,2
$log\, g$	3.5±0.2	1
$[Fe/H]$	-0.5±0.2	1
M_*	5.2±0.2 $M_\odot$	1
R_*	$7.6\pm^{0.6}_{2}$ $R_\odot$	1
L_*	$640\pm^{130}_{160}$ $L_\odot$	1
age	5×10^5 yr	1
M_V	-1.75±0.3 mag	1
m_V	6.77 mag	3
A_V	0.3	3
m_K	4.28	4
$F_{obs}(K)/F_*(K)$	4.3	1
i	20°	5
$v_{rot}\, sin\, i$	50±3 km s^{-1}	6
$\dot{M}_{acc}$	9×10^{-7} $M_\odot$ yr^{-1}	4 + 1

References. (1) This work; (2) Thé et al. (1994); (3) Manoj et al. (20 (4) Garcia Lopez et al. (2006); (5) Hales et al. (2014); (6) Alecian (2013);

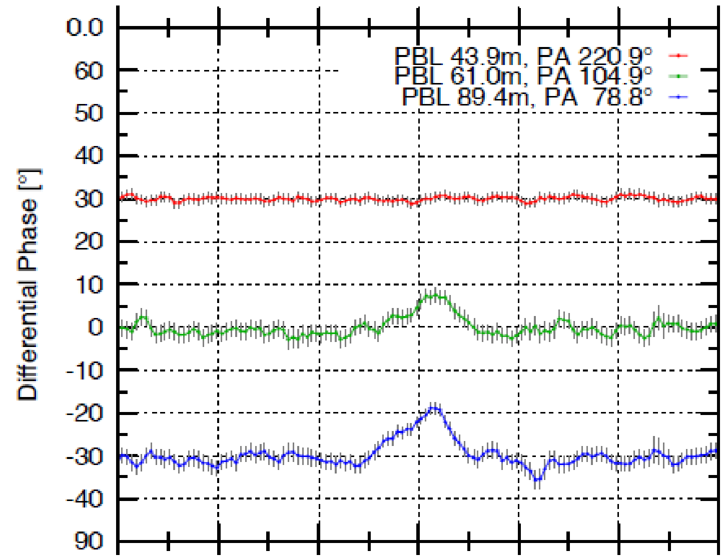

Parameter[a]	Range of Values	Model P5
T_e (K)	8000–10 000	10 000
Half opening angle (θ_1)	20°–60°	30°
Inner radius - $\omega_1(R_*)$	2–3 (0.07–0.1 AU)	3 (0.1 AU)
Outer radius - $\omega_N(R_*)$	4–30 (0.13–1 AU)	30 (1 AU)
Acceleration parameter (β)	3–5	5
Mass load parameter (γ)	3–5	3
Mass loss rate - $\dot{M}_w(M_\odot\, yr^{-1})$	10^{-8}–2×10^{-7}	2×10^{-7}

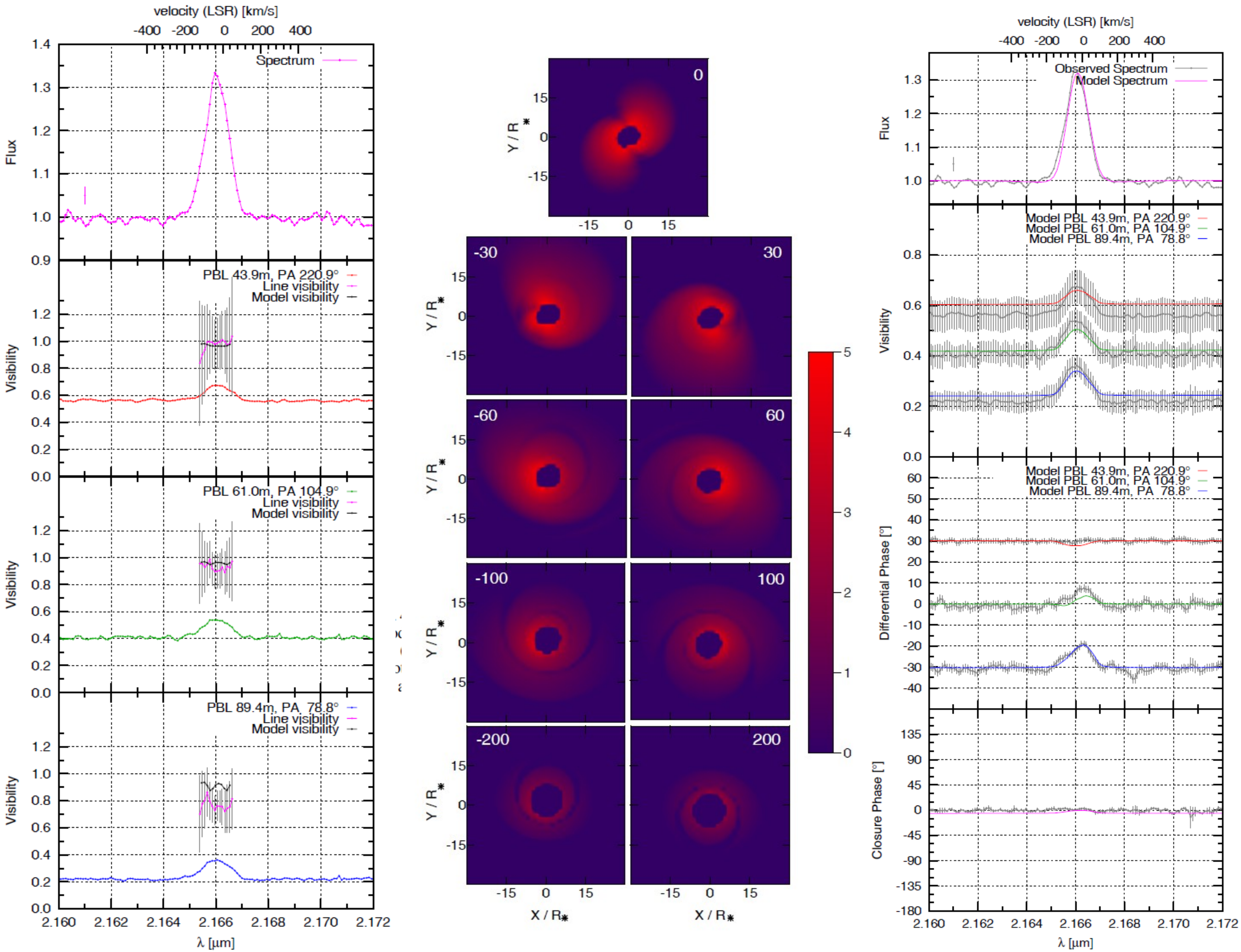

Fi
ca
(a
mi
tic
sh

Conclusion

- The disk wind of Herbig Ae stars differs from that of T Tauri stars by the larger opening angle due to the action of the radiation pressure.
- The disk wind of Herbig Ae stars contributes substantially to the hydrogen emission spectra of these stars; nevertheless, the region of the magnetosphere is also a source of the emission and has to be taken into account.
- Combination of the disk wind parameters and inclinations permits us to obtain a large variety of profile shapes.
- Calculation of the interferometric functions together with the emission lines modeling gives constraints to the wind parameters and provides us an additional information about the star+disk system
- “The Brackett γ enigma” remains an open issue

Hydrogen lines as a diagnostic tool for studying multicomponent emitting regions in hot young stars: magnetosphere, X-wind, and disk wind

L.V. Tambovtseva[1], V. P. Grinin[1,2], and G. Weigelt[3] (A&A 2014)

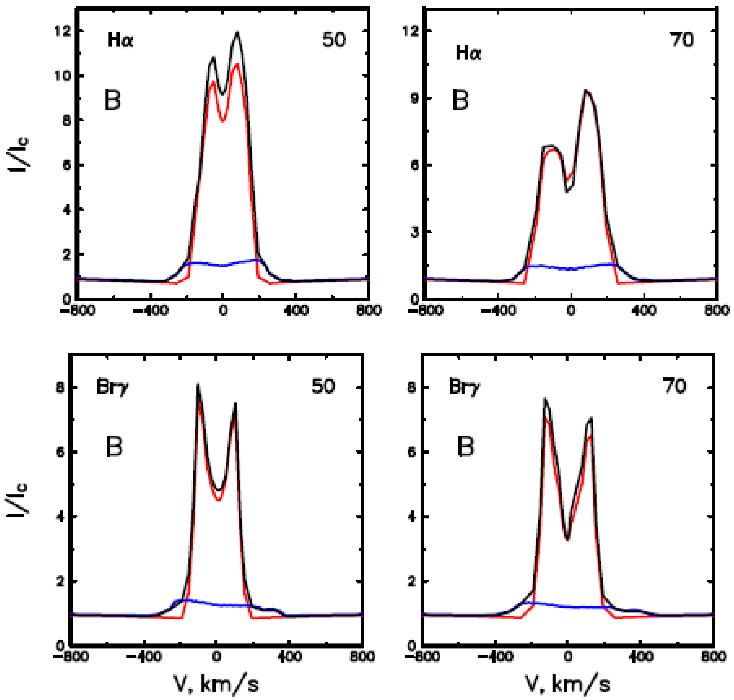

Hα

Brγ

Magnetosphere

Disk wind

Total